Fixed-bed Column Study of Textile Dye Direct Blue 86 by using A Composite Adsorbent

Monal Dutta, Jayanta Kumar Basu*, Md Hassan Faraz, Nitin Gautam and Adarsh Kumar

Indian Institute of Technology, Kharagpur, India

_____

ABSTRACT

In the present study, the adsorption of a textile dye direct blue 86 was studied through a fixed-bed column by using a carbon-alumina composite pellet. The adsorbent was developed by using microwave assisted activated carbon and commercial alumina. In order to find out the batch adsorption characteristics various adsorption isotherms such as, Langmuir, Freundlich and Tempkin were investigated and the corresponding monolayer capacity was found to be 500.16 mg/g. The fixed – bed column was used to investigate the dynamic adsorption characteristics where the effects inlet dye concentration (50–200 mg/L), feed flow rate (5 – 15 mL/min) and activated carbon bed height (5.04 – 10.16 cm) on the adsorption breakthrough were also investigated. The maximum removal capacity in the column study was found to be 142.67 mg/l with an initial dye concentration and flowrate of 100 mg/l and 12 ml/min according to Bohart-Adams model. The breakthrough behavior was also effectively described by the Yoon-Nelson and Clark model.

Keyword: Direct blue; Carbon alumina palette; Equilibrium study; Column study; Bohart-Amams model; Yoon-Nelson model; Clark model.

_____

INTRODUCTION

In the recent era of technological and industrial advancement, the introduction of various colored compounds into different water bodies cause severe imbalance to aquatic environment [1, 2]. These colored substances are mainly originated from different textile, leather, paper, food and cosmetic industries. It has been estimated that over 7×10^5 tons of dyes produced annually worldwide and nearly 2% of these dyes are discharged directly into the water bodies which may prove detrimental to aquatic life due to the presence of metals and chlorides in them [3]. Moreover dyes may be mutagenic or carcinogenic and if contacted, can cause severe damage to human beings such as malfunction of kidney, reproductive system, liver, brain and central nervous system. [4]. Among such dyes Direct Blue 86 (DB 86) is a well known anionic dye used for various purposes such as dyeing of cellulosic fibers like cotton, flax, viscose rayon, acetate and jute. It is also applicable for leather and paper coloration. Waste water containing dyes cannot be treated easily as they are chemically very stable. Hence they need to be removed. Various removal technologies like adsorption, photo-degradation, coagulation, flocculation, chemical oxidation, electro-chemical oxidation, biological process etc. are available for the removal of dye from the wastewater [5, 6]. But adsorption by activated carbon is worth mentioning amongst all because of its ease of processing and ability to adsorp a large variety of adsorbate [7]. Commercial activated carbon is widely used to remove various adsorbates but its high cost limits its widespread use. Therefore, search for an alternative low cost raw material for making activated carbon has become very important now a day. In the present investigation, an activated carbon was developed from the scrap

882

_____

wood of Acacia Auriculiformis for the removal of textile dye Direct Blue 86 (DB 86). Generally, in the batch adsorption study the adsorbent is used in its powdered form which has the great disadvantage of separation after being used. To overcome this difficulty, the carbon may be used in its pelletized form. On the other hand, a continuous flow process using a packed bed is more advantageous for the treatment of waste water on a large scale. A lot of literature is already available on the batch adsorption study but none on fixed bed adsorption of a textile dye using Acacia Auriculiformis as the precursor material for activated carbon. Therefore, in the present study, the adsorption characteristics of DB 86 were investigated in a fixed bed column by using microwave assisted activated carbon. The effects of different process parameters such as, dye flowrate, bed height and inlet dye concentration on the breakthrough pattern were also investigated. The adsorption breakthrough behavior was analyzed by using Yoon-Nelson, Clark and Bohart-Adams' model.

MATERIALS AND METHODS

2.1. Raw materials
The scrap wood of Acacia Auriculiformis selected for this work, was collected from local saw mill. Hydrochloric acid and ammonia were procured from Merck Specialities Private Limited, Mumbai, India.

2.2. Preparation of activated carbon
The char was prepared by carbonization of Acacia Auriculiformis scrap wood in an inert atmosphere. The wood scrap was first cut into small pieces of 2 mm width and 40 mm of length, cleaned with distilled water and was sun dried for 24 h prior to the carbonization. The wood pieces were kept on a ceramic boat which was placed at the center of a 40-mm i.d tubular furnace. The material was then heated from ambient temperature to the carbonization temperature of 750 °C at the rate of 4 °C/min in a continuous flow of N_2 (300 ml/min) and then it was kept at this temperature for 1h for subsequent activation. It was then allowed to cool to ambient temperature in presence of N_2 flow. The char (C750N) was sieved to obtain the desired size fractions and stored in a desiccator over silica gel. The C750N was further activated in a domestic microoven (IF20PG3S) for five minutes at a constant input power of 800 W and a frequency of 2450 MHz. After treating in the microoven C750N was termed as AC750NMW5.

2.3 Preparation of the composite adsorbent
 Microwave assisted activated carbon (AC750NMW5) and commercial alumina powder was mixed thoroughly with PVA in a weight ratio of 2:2:1.5. Then, the slurry was prepared by adding a small quantity of water which was then heated up to 90 °C for 30 min in a constant temperature water bath and the heating process was carried out till a sticky mass was formed. Then the sticky mass was shaped into spherical pallets. The pellets were kept overnight in an air oven at 110 °C and placed in tubular furnace where these were heated up to 300 °C for 2 h in a flow of nitrogen (300 ml/ min). The pellets were kept at to 300 °C for 1 h for subsequent activation. The resulting pellets were then cooled to room temperature and stored in a desiccator over silica gel. The prepared pellets were termed as carbon-alumina composite pallets (CACP).

2.4. Characterization of activated carbon
  The surface area and the total pore volume of the prepared char and the activated carbon were determined by using N_2 adsorption-desorption method by using Brunauer Emmett Teller (BET) apparatus (Autosorb-1, Quantacrome).

2.5. Equilibrium and kinetic study of DB-86
The monolayer adsorption capacity of the prepared char for direct blue-86 (DB-86) was determined by the equilibrium study. The equilibrium study was carried out by adding 0.1 g of adsorbent into a series of 250 ml conical flask containing 100 ml solution of direct blue 86 and was shaken for 36 h at room temperature. After this the samples were centrifuged and the concentrations were analyzed in a UV-Vis spectrophotometer. The kinetic study was carried out by analyzing adsorptive uptake of the dye from aqueous solution at different time intervals. The adsorptive capacity of different adsorbents was compared through batch adsorption. The equilibrium adsorption capacity was calculated from the relationship

$$q_e = \frac{(C_0 - C_e)}{w}V$$

(1)

_____

Where, q_e (mg/g) is the equilibrium adsorption capacity, C_e is the dye concentration at equilibrium (mg/l/), *V* is the volume of solution (l) and *w* is the weight of adsorbent (g).

2.6. Experimental set-up
The fixed-bed column was made of Pyrex glass tube of 1.3cm inner diameter and 17 cm height. The column was packed with CACP followed by a layer of glass beads on both the side to provide uniform flow of solution. To avoid entrapping of air bubbles inside the CAC pellets, the particles were soaked in appropriate amount of water and agitated until no air bubbles were detected in the solution. A known quantity of the prepared adsorbent was packed in the column to yield the desired bed height of 2.54, 7.62 and 10.16 cm. Dye solution of known concentrations (50, 100 and 200 mg/L) at pH 1.5 was allowed to flow through the column at a desired flow rate of 5, 10 and 15 mL/min. The aliquot of the DB-86 solution was collected at the outlet of the column at regular time intervals and the residual dye concentration was measured using a double beam UV–visible spectrophotometer (Spectra scan UV 2600, Chemito, India).at 619 nm. All experiments were carried out at temperature of 28±1 ∘C.

2.7. Analysis of fixed-bed column data
The dynamic adsorption characteristics in a fixed-bed column were studied through analyzing the shape of the experimental breakthrough curves. The experimental breakthrough curves show the loading behavior of the adsorbate on a fixed-bed column. They are generally expressed in terms of normalized dye concentration, defined as the ratio of instantaneous or outlet adsorbate concentration to the initial adsorbate concentration (C_t/C_0) as a function of time for a given bed height or adsorbate flowrate [8]. The effluent volume (V_{eff}) can be calculated as

$$V_{eff} = Qt_{total} \qquad\qquad\qquad (2)$$

Where, t_{total} and Q are the total time taken for the flow of adsorbent (min) and volumetric flow rate (mL/min). The total amount of dye adsorbed q_{total} (mg) for a given bed height, feed concentration and flow rate is can be determined as:

$$q_{total} = \frac{Q}{1000} \int_{t=0}^{t=tt_{otal}} C_{ad}\,dt \qquad\qquad\qquad (3)$$

Besides, the equilibrium uptake q_{eq} (mg/g) or maximum capacity of the column can be calculated as [9]:

$$q_{eq} = \frac{q_{total}}{w} \qquad\qquad\qquad (4)$$

Where, q_{total} and w are the the total amount of dye adsorbed (q_{total}) and amount of adsorbent (mg).

2.8. Data analysis
The experimental data were analyzed using Origin Pro (version 8) computer software. The goodness of fit was measured through the regression coefficient (R^2).

RESULTS AND DISCUSSION

3.1. Characterization of the prepared adsorbents
The BET surface area (S_{BET}), total pore volume (V_{tot}) and average pore size of C750N and AC750NMW5 were determined from the physical adsorption data of N_2 at 77 K and the values are shown in Table 1. It can be seen from Table 1 that AC750NMW5 has the highest surface area and total pore volume. Inside the microoven a high temperature could be reached in comparatively shorter period of time resulting dissipation of huge amount of energy at a molecular level. Consequently, the roughness of the pore walls may also be increased due to rapid heating with the formation of additional active sites [10]. Besides, rapid heating could accelerate the release of tar or volatile matter from the pore interior which results into higher pore volume [11].

_____

Table-1: Comparison of surface properties of C750N and AC750NMW5

Adsorbent	Surface area (m^2/g)	Total pore volume (cc/g)	Average pore diameter (Å)
C750N	514.2	0.36	27.99
AC750NMW5	695	0.50	28.55

3.2. Equilibrium studies of DB-86 using AC750NMW5
In order to investigate the adsorption characteristics the experimental data were fitted to Freundlich, Langmuir, Tempkin and Harkins-Jura isotherms and the corresponding equilibrium plot is shown in Fig. 1.
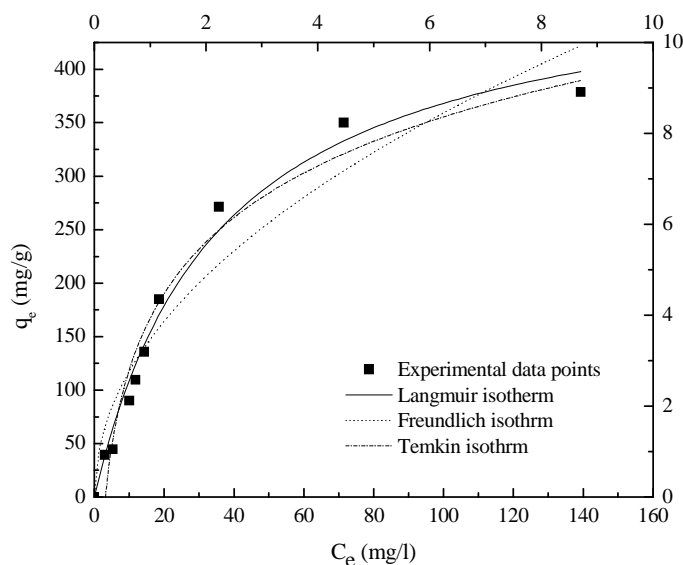
Fig. 1. **Equilibrium isotherm for Db 86**

The Langmuir isotherm represents the uni-molecular adsorption of the adsorbate molecule on the adsorbent surface [12]. The model can be expressed as:

$$\frac{1}{q_e} = \frac{1}{K_l Q_0} + \frac{1}{Q_0} \tag{5}$$

Where, q_e is the equilibrium adsorption capacity, C_e is the equilibrium dye concentration, K_1 is the Langmuir constant related to the energy of adsorption (l /mg) and Q_0 is the maximum amount of adsorption corresponding to complete the monolayer coverage on surface (mg/g). The experimental data fitted to Langmuir model and the corresponding monolayer adsorption capacity was 500.16 mg/g. Similarly, the Freundlich isotherm can be used for non-ideal sorption that involves heterogeneous surface energy systems [13] and is expressed by the following equation:

$$\log q_e = \log K_F + \frac{1}{n} \log C_e \tag{6}$$

Where, K_F is a rough indicator of the adsorption capacity and $1/n$ is the adsorption intensity. In general, with the increase of the adsorption capacity K_F value increases. The Tempkin isotherm describes the heat of adsorption and interaction between adsorbent-adsorbate molecules [14]. The Tempkin isotherm can be expressed as:

$$q_e = B_1 \ln k_T + B_1 \ln C_e \tag{7}$$

Where, k_T and B_1 are Tempkin isotherm constant. The parameters values of different isotherms are shown in Table 2.

885

_____

Table 2 Equilibrium model parameters

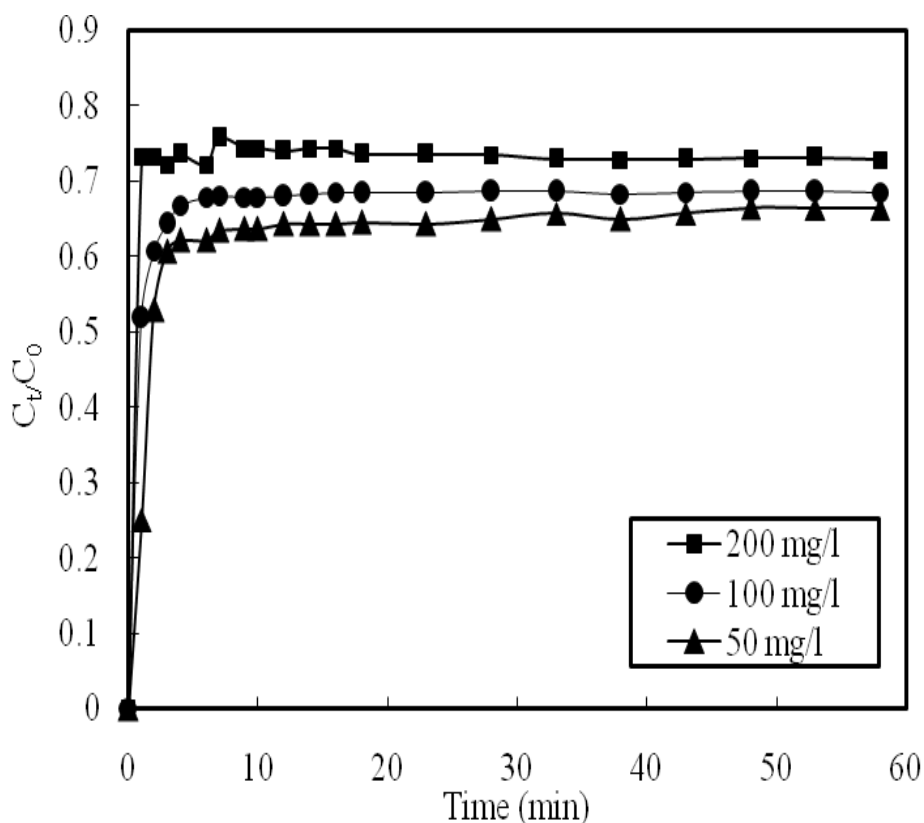| Isotherm model	Kinetic parameters
Freundlich $$q_e = K_F C^{1/n}$$	K_F = 38.36; n = 2.06; R^2 = 0.93; χ^2 = 1372.66
Langmuir $$qe = \frac{K_l q_m C_e}{1 + K_l C_e}$$	K_l = 0.03; Q_0 = 500.16; R^2 = 0.98; χ^2 = 295.0
Tempkin $$q_e = K_m \log(h C_e)$$	Km = 0.32; B = 102.59; R^2 = 0.96; χ^2 = 677.67

Fig. 2. Breakthrough curves for DB 86 adsorption at different inlet concentrations (bed height = 7.62 cm, flow rate = 12mL/min, temperature = 28±1 ∘C).

3.3. The fixed-bed study
3.3.1. Effect of initial dye concentration
The effect of initial dye concentrations was studied by varying the dye concentration from 50 – 200 mg/l with an adsorbent bed height of 7.62 cm whereas the flowrate was kept constant at 12 ml/min. The effect of initial concentration is shown in Fig. 2 by the adsorption breakthrough curve. It was seen from Fig. 2 that the value of Ct/Co increased from 0.66 to 0.73 with an increase in inlet concentration from 50 to 100 and 200 mg/l. It was further observed that the breakthrough time slightly decreased with increasing inlet dye concentration. This may be

_____

attributed to the fact that at lower inlet concentrations, breakthrough occurred slowly but with increase in inlet concentration the breakthrough time decreased. The driving force for mass transfer was also increased with increase in inlet dye concentration which in turn increased the adsorption capacity. Conversely, the rate of mass transfer got reduced at lower inlet concentration resulting into slower transport. Therefore it can be concluded that the adsorption process is concentration dependent [15]. Similar results were obtained for biosorption of reactive black by bamboo waste based activated carbon [16] and for the removal of acid dye using pristine and acid-activated clays [17].

3.3.2. Effect of the solution flow rate
The adsorbate flowrate had a significant effect on DB-86 adsorption in the fixed bed column. The effect of flowrate was shown in Fig. 3 with the help of experimental breakthrough curve. The flow rate was varied from 12 – 15 ml/min with a constant bed height and initial concentration of 7.62 cm and 100 mg/l respectively. It was seen from Fig. 3 that breakthrough occurred at comparatively faster rate at higher adsorbate flowrate and less time was taken to reach the saturation breakthrough. The possible reason may be at higher adsorbate flowrate DB-86 had less time to contact with the activated carbon bed which resulted into steeper breakthrough curve. This phenomenon can also be explained in the vicinity of mass transfer fundamentals. The rate of mass transfer gets increased at higher flowrate leading to faster saturation [18]. Conversely, the adsorption capacity is decreased with increase in flowrate due to shorter residence time of the adsorbate molecule in the fixed bed column. Therefore, the surface of the activated carbon never gets saturated with the adsorbate molecules and as a result the equilibrium never reached. The results obtained in the present investigation are in well agreement with the results obtained by Zulfadhly et al. [19] where macro fungus *Pycnoporus sanguineus* was used to adsorb heavy metals (Pb, Cu and Cd) from aqueous solution in fixed-bed column at various flow rates.
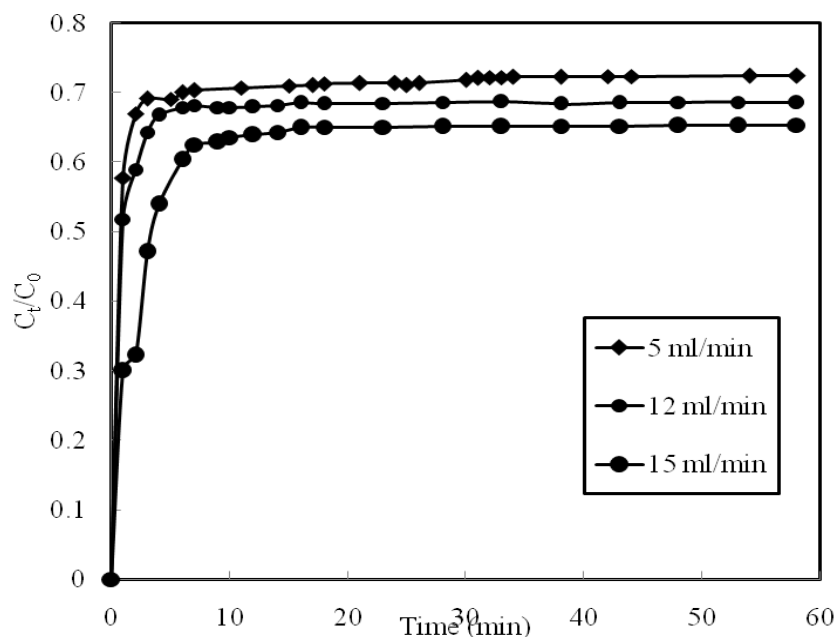

Fig.3. Breakthrough curves for DB 86 adsorption at different flow rates (inlet Db 86 concentration = 100 mg/L, bed height = 7.62 cm, temperature = 28±1 ∘C).

3.3.3. Effect of activated carbon bed height
The effect of bed height is shown in Fig.4. The effect of bed height was studied at an initial dye concentration of 100 mg/l and a flowrate of 12 ml/min respectively. The Bed height was varied from 5.02 – 10.16 cm. It was seen from the breakthrough curve that the slope of breakthrough curve decreased with increasing bed height. It may be because of the reason that with the increase in bed height the adsorbate has more time to contact with the activated carbon which in turn results into higher removal capacity and lower solute concentration in the effluent. Besides, at higher bed height the availability of the effective surface area of adsorbent is more which offers more active sites to adsorption and it also broadens the mass transfer zone length [20].
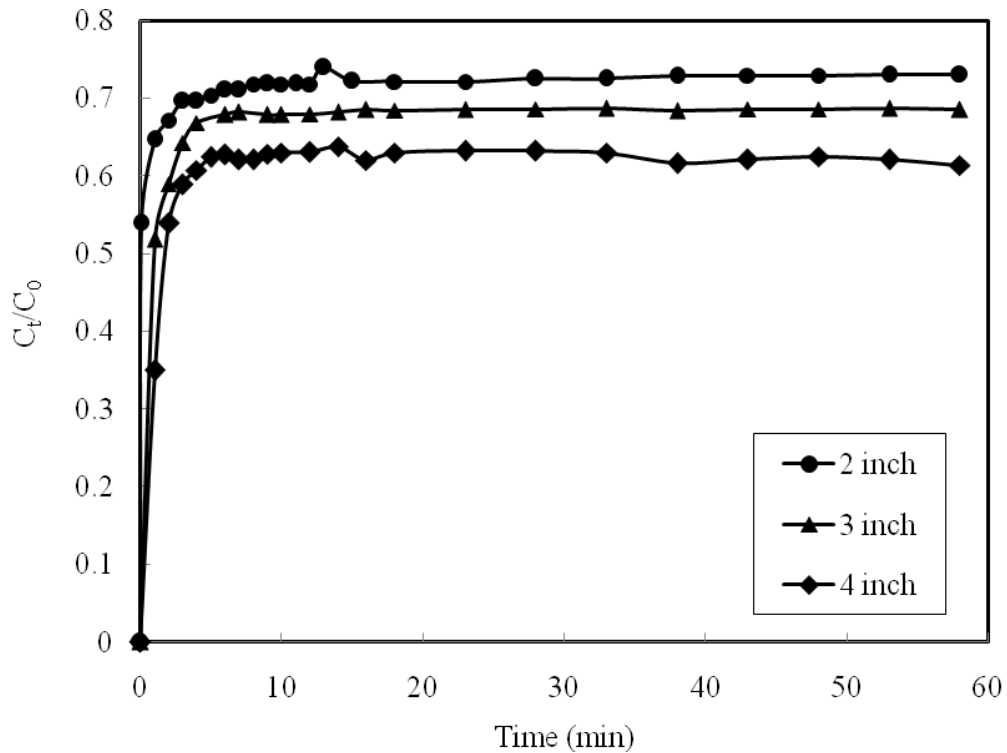
_____

Fig. 4. Breakthrough curves for DB 86 adsorption on prepared BGAC at different bed heights (inlet DB 86 concentration = 100 mg/L, flow rate = 12 mL/min, temperature = 28±1 ∘C).

3.4. The Bohart-Adams Model
The Bohart-Adams model is widely used for designing fixed bed column. The model is based on surface reaction theory [21] and according to this model the rate of adsorption is proportional to fraction of adsorption capacity that still remains on the surface of the adsorbent [22]. The Bohart and Adams' model describes a fundamental relationship between the normalized concentration (C_b/C_0) and the bed height (Z) and the relationship can be described by the following equation:

$$t_b = \frac{N_0 Z}{C_0 v} - \frac{1}{k_{AB} C_0} \ln(\frac{C_0}{C_b} - 1)$$

(7)

where, C_0 and C_b are the initial and breakthrough concentration in mg/l respectively, k_{AB} is the Bohart Adams, model constant (l/mg-min), N_0 is the adsorption capacity of the adsorbent in mg/l, Z is the bed depth in cm, v is the linear velocity in cm/min and t_b is the breakthrough time (min). The above equation can be written in a linear form as

$$t_b = aZ + b$$

(8)

where,
$$a = \frac{N_0}{C_0 v}$$

(9)

$$b = \ln\left[(\frac{C_0}{C_b}) - 1 \right] \times \frac{1}{C_0 k_{AB}}$$

(10)

_____

 The iso-removal lines are constructed by plotting different bed heights (5.08, 7.62 and 10.16 cm) against breakthrough times at constant flowrate (12 ml/min) and initial dye concentration (100 mg/l) as shown in Fig. 5. The adsorption capacity (N_0) and the rate constant of adsorption (k_{AB}) were calculated from the slope and intercept of the isothermal lines.
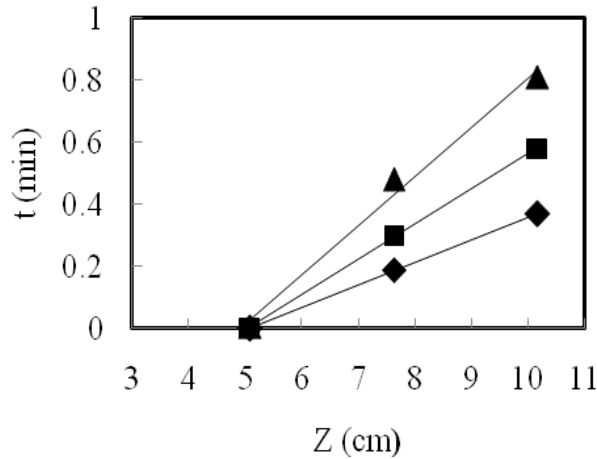

Fig. 5. Bohart-Adams plot at different adsorption breakthrough

The values of N_0 and k_{AB} which can be further used in column design are shown in Table 3. Therefore, by using the respective linear equation, the breakthrough time for a particular bed height for new feed concentration or flowrate can be predicted easily [23].

Table 3 The Bohart-Adams model constants for the fixed bed column study

Iso-removal Percentage	a_i (min/cm)	b_i (min)	N_0 (mg/l)	k_{AB} (l/minmg)	R^2
10	0.072	-0.366	65.02	0.0600	0.999
20	0.113	-0.571	102.04	0.0385	0.999
30	0.158	-0.775	142.67	0.0284	0.989

The modified slope (a_f) for a new feed concentration was calculated directly by multiplying the original slope (a_i) by the ratio between the original (C_0) and new feed concentration (C_f).

$$a_f = a_i \left(\frac{C_0}{C_f} \right)$$
(11)

The modified intercept was also calculated by the following equation

$$b_f = b_i \left(\frac{C_0}{C_f} \right) \left[\frac{\ln(C_f - 1)}{\ln(C_0 - 1)} \right]$$
(12)

where, b_i and b_f are the original and modified intercept for a new feed concentration.

Similarly the modified slope constant for a new flowrate was calculated as

_____

$$a_f = a_i \left(\frac{V_0}{V_f} \right)$$

(13)

where, V_0 and V_f are the original and new flow rate. The predicted breakthrough time calculated from the above equations was compared with observed breakthrough time and the corresponding values are shown in Table 4 and 5.

Table 4 Predicted breakthrough time form Bohart-Adams constant for a new feed concentration Break point (%)

Break point (%)	a_i	b_i	C_0	C_f	C_0/C_f	a_f	b_f	Z	t_{Pred}	t_{Obs}
10	0.072	-0.366	100	50	2	0.144	-0.62	7.62	0.47	0.41
20	0.113	-0.571	100	50	2	0.266	-0.97	7.62	1.06	0.85
30	0.158	-0.775	100	50	2	0.316	-1.31	7.62	1.09	1.10
10	0.072	-0. 366	100	200	0.50	0.036	-0.21	7.62	0.06	0.08
20	0.113	-0.571	100	200	0.50	0.057	-0.33	7.62	0.10	0.17
30	0.158	-0.775	100	200	0.50	0.079	-0.45	7.62	0.15	0.28

A high value of regression coefficient was obtained when these predicted values of breakthrough time were plotted against the observed values of breakthrough time. Therefore, model developed can be further utilized for modeling of a contentious column under different experimental conditions such as varying flow rates and feed concentrations.

3.5. Yoon-Nelson and Clark Model
This model is based on the assumption that the rate of decrease in the probability of adsorption for each adsorbate molecule is proportional to the probability of adsorbate adsorption and the probability of adsorbate breakthrough on the adsorbent [24]. The Yoon-Nelson model is less complicated than other models. The linearized form of the Yoon-Nelson model for a single component system is expressed as:

$$\ln \frac{C_t}{C_0 - C_t} = k_{YN} t - \tau k_{YN}$$

(14)

where, k_{YN} is the rate constant (min^{-1}) and τ (min) is the time required for 50% adsorbate breakthrough. The values of k_{YN}, τ, χ^2 and R^2 are shown in Table 6 were determined from the from the slope and intercept of the linear plot of $\ln [C_t /(C_0 - C_t)]$ and t according to Eq. (13). The 50% breakthrough time (τ) was increased with increasing feed concentration (C_0) and bed height (Z). Besides, the rate constant (k_{YN}) was increased with decreasing feed concentration and increasing bed height. The results obtained were in a good agreement with the experimental results of Ahmad et.al.

Table 6 Parameters for Yoon-Nelson under different experimental conditions

Concentration (mg/l)	bed height (cm)	Flowrate (ml/min)	k_{YN}(1/min)	T (min)	R^2	χ^2
100	7.62	12	0.214	0.488	0.95	2.2×10^{-4}
100	5.08	12	0.15	0.28	0.80	1×10^{-3}
100	10.16	12	0.13	0.72	0.87	1.6×10^{-4}
50	7.62	12	0.218	0.47	0.93	3.2×10^{-4}
100	7.62	5	0.354	0.04	0.99	1.0×10^{-4}
100	7.62	15	0.364	3.56	0.90	0.023

3.6. Clark Model
The Clark model introduces a new procedure to simulate the breakthrough curves by using the Freundlich isotherm constant [26]. The linearized form of the model can be represented as,

$$\ln \left[\left(\frac{C_0}{C_t} \right)^{n-1} - 1 \right] = -rt + \ln A$$

(15)

where, r (min^{-1}) and A are the Clark model parameters.

890

_____

The predicted model parameters calculated using a Freundlich constant of n = 2.06 are shown in Table 7. It was seen from Table 7 that values of r increased with decrease in bed height. Besides, the value of A also increased with increase in bed height.

Table 7 Clark model under different experimental conditions

Initial concentration (mg/l)	Bed height (cm)	Flow rate (ml/min)	r (l/min)	A	R^2	$X^2(10^4)$
100	5.08	12	0.114	0.74	0.99	310
100	7.62	12	0.262	1.29	0.99	6.9
100	10.16	12	0.141	1.19	0.87	28.8
100	7.62	5	0.318	1.03	0.96	43.5
100	7.62	15	0.122	1.49	0.99	4.98

CONCLUSION

The adsorption of a typical textile dye direct blue 86 was studied through a fixed bed column. A carbon-alumina composite adsorbent was developed for this purpose. The activated carbon was developed by microwave activation. The monolayer adsorption capacity according to Langmuir isotherm was found to be 500.16 mg/g. The dynamic adsorption characteristics for DB 86 adsorption were investigated by using a ixed bed column. The effects of various parameters such as initial dye concentration, adsorbate flow rate and adsorbent bed height on the breakthrough were also investigated. The maximum bed capacity was found to be 142.67 mg/l. The experimental breakthrough data were fitted to Bohart Adams', Yoon-Nelson and Clark model. It was seen from Bohart Adams' model that with an increase in percentage breakthrough the values of N_0 increased from 65.02 – 142.67 mg/l respectively.

REFERENCES

[1] D. Charumathi, N. Das, *Desalination*, **2011**, 285, 5-9.
[2] Y. Yao, F. Xu, M. Chen, Z. Xu, Z. Zhu, *Bioresour Technol*., **2010**, 101, 3040.
[3] D. Xu, S. Hein, S.L. Loo, K. Wang, *Ind. Eng. Chem. Res*., **2008**, 47, 8796–8800.
[4] K. Kadirvelu, C. Karthika, N. Vennilamani, S. Pattabhi, *Chemosphere*, **2005**, 60, 1009–1017.
[5] A. Adak, M. Bandyopadhyay, A. Pal, *Dyes Pigm*., **2006**, 69, 245-251.
[6] V. Ponnusami, R. Madhuram, V. Krithika, S.N. Srivastava, *Chem. Eng. J.,* **2008**, 140-609.
[7] M. Rafatullah, O. Sulaiman, R. Hashim, A. Ahmad, *J. Hazard. Mater*., **2010**, 177, 70.
[8] J. Guo, A.C. Lua, *Mater. Chem. Phys*. 80 (**2003**) 114–119.
[9] Z. Aksu, F. Gonen, *Process Biochem*. **2004**; 39:599–613.
[10] L. Huang, Y. Sun, W. Wang, Q. Yue, T. Yanga, *Chem. Eng. J*., **2011**, 171(3), 1446-1453.
[11] Q.S. Liu, T. Zheng, P. Wang, L. Guo, *Ind. Crops Prod*., **2010**, 31, 233–238.
[12] J. Song, W. Zou, Y. Bian, F. Su, R. Han, *Desalination*, **2010**, 265(1-3), 119–125.
[13] N. Ozturk, D. Kavak, *J. Hazard. Mater*., **2005**, B127, 81–88.
[14] A. Ergene, K. Ada, S. Tan, H. Katırcıoğlu, *Desalination*, **2009**, 249(3), 1308–1314.
[15] J. Goel, K. Kadirvelu, C. Rajagopal, V.K. Garg, *J. Hazard. Mater*. B., **2005**, 125, 211–220.
[16] A.A. Ahmad, B.H. Hameed, *J. Hazard. Mater*., **2010**, 175, 298–303.
[17] S.H. Lina, R.S. Juangb, Y.H. Wang, *J. Hazard. Mater*., **2004**, B113, 195–200.
[18] K. D.C.K. Porter JF, G. McKay, *Chem. Eng. Sci*., **2000**, 55, 5819–5829.
[19] Z. Zulfadhly, M.D. Mashitah, S. Bhatia, *Environ. Pollut*., **2001**, 112, 463–470.
[20] K. Vijayaraghavan, J. Jegan, K. Palanivelu, M. Velan, *J. Hazard. Mater*., **2004**, 113B (1–3), 223–230.
[21] B. Kiran, A. Kaushik, *Chem. Eng. J.,* **2008**, 144(3), 391-399.
[22] M. Lehmann, A.I. Zouboulis, K.A. Matis, *Environ. Pollut*., **2001**, 113(2), 121-128.
[23] Y.H. Yoon, J. H. Nelson, *Am. Ind. Hyg. Assoc. J.,* **1984**, 45, 509-516.
[24] S. Singh, V.C. Srivastava, I.D. Mall, *Coll. Surf. A: Physicochem. Eng. Asp*., **2009**, 332(1), 50-56.
[25] A.A. Ahmad, B.H. Hameed, *J. Hazard. Mater*., **2010**, 175(1-3), 298-303.
[26] F.A. Batzias, D.K. Sidiras, *Bioresour. Technol.,* **2007**, 98(6), 1208–1217.